

## Cluster expansion technique: An efficient tool to search for ground-state configurations of adatoms on plane surfaces

R. Drautz, R. Singer, and M. Fähnle\*

*Max-Planck-Institut für Metallforschung, Heisenbergstrasse 3, D-70569, Stuttgart, Germany*

(Received 23 September 2002; published 27 January 2003)

The cluster expansion technique is applied to describe the energetics of adatom configurations on plane substrate surfaces at submonolayer coverage and to find the stable configuration in thermodynamic equilibrium. The power of the method is demonstrated for the case of Li adatoms on Mo(112).

DOI: 10.1103/PhysRevB.67.035418

PACS number(s): 68.43.Hn, 61.46.+w, 64.70.Nd

In the past years there has been much progress in nanotechnology; i.e., it has become possible to design materials on atomic scale, plane by plane, row by row, and atom by atom.<sup>1</sup> The final objective is to tailor nanostructured materials in such a way that new physical features arise. These may be interesting from a fundamental point of view, e.g., the formation of Peierls-like instabilities and unusual non-Fermi-liquid ground states in one-dimensional metals<sup>2</sup> or the features of magnetism in one-dimensional chains.<sup>3</sup> There may be also interesting technological applications in the field of microelectronics, e.g., for the design of memories for data storage with magnetic elements on a nanoscale<sup>1</sup> or even with single atoms that store a bit.<sup>4</sup>

One of the routes to nanostructures is the deposition of adatoms on stepped or plane substrate surfaces. The type of structures (e.g., dots or chainlike structures or two-dimensional structures, etc.) which will form on a plane surface depends on the interaction of the adatoms with each other and with the substrate atoms. For instance, by use of strongly anisotropic surfaces like (110) fcc and (112) bcc surfaces it is possible to grow chainlike structures for certain combinations of adatoms and substrates, e.g., for Cu on Pd(110) (Refs. 5 and 6) or for Li on Mo(112) (Refs. 7 and 8). In many cases the obtained adatom structures are metastable and determined by the kinetics of diffusion-controlled aggregation.<sup>5</sup> In other cases, e.g., Li on Mo(112),<sup>7</sup> the chainlike structures represent the thermal equilibrium configuration.

For the design of nanostructures on plane surfaces in thermal equilibrium it would be extremely helpful to have rule-of-thumb guidelines telling which combination of adatoms and substrate atoms should be used to stabilize the various desired geometries of the nanostructures. To find such guidelines, many experimental and theoretical investigations for many different systems are required. The already existing theoretical investigations can be subdivided into two groups. The calculations of the first group (see, e.g., Ref. 6) are based on  $N$ -body potentials which allow one to sample with a reasonable calculational effort many different competing configurations or to search for the minimum energy configuration by means of molecular-dynamics studies. The basic idea of the calculations of the second group (e.g., Ref. 8) is that a highly accurate and reliable determination of the energies of the configurations requires the use of the *ab initio* density functional theory. The price one has to pay is that the calculations are very time consuming so that only a rather limited

number of configurations can be sampled. It is the objective of the present paper to demonstrate that this problem of the *ab initio* electron theory can be overcome when combining it with the cluster expansion (CE) technique.<sup>9</sup> So far this technique has been used mainly to determine the ordering phenomena of alloys and compounds in the bulk (see, e.g., Ref. 10) and at the surface.<sup>11</sup> In the present paper we apply it to describe the configurations formed by adatoms on plane surfaces at submonolayer coverage where there is at most one atom above each lattice site. Former approaches to deal with such situations also represented the configurational energies in terms of contributions from cluster figures.<sup>12</sup> However, they considered from the very beginning only a small number of different clusters and did not make clear contact with the completeness relation provided by the CE technique which guarantees the predictive power of the CE technique.

In the following we consider situations where the adatoms occupy only one type of available surface sites for all coverages  $\Theta$  with  $0 \leq \Theta \leq 1$  (of course, the method can be extended to the case where several types of lattice sites are involved). Furthermore, we assume that there are no adatom-induced surface reconstructions. The available surface sites are labeled by the index  $i$ , and they form a two-dimensional lattice. A “spin” variable  $\sigma_i$  is assigned to each lattice site which exhibits the value of 1 if the site is occupied by an adatom and  $-1$  otherwise. If the surface lattice contains  $N$  sites, each configuration of adatoms is characterized by a configuration vector  $\boldsymbol{\sigma} = (\sigma_1, \sigma_2, \dots, \sigma_N)$ . According to Ref. 9 the energy  $E(\boldsymbol{\sigma})$  may be completely described by a sum of contributions arising from all possible spin clusters  $\alpha$  on the surface lattice,

$$E(\boldsymbol{\sigma}) = \sum_{\alpha} J_{\alpha} \Phi_{\alpha}(\boldsymbol{\sigma}). \quad (1)$$

In Eq. (1) the index  $\alpha$  labels the various different cluster figures, i.e., isolated atoms, nearest-neighbor pairs and further distant pairs, triplets of different shapes, quartets, and so on [Fig. 1(a)]. The  $\Phi_{\alpha}$  are given by products of the spin variables which form the cluster, i.e.,

$$\Phi_{\alpha} = \prod_{i \in \alpha} \sigma_i, \quad (2)$$

and the  $J_{\alpha}$  are the corresponding interaction parameters which do not depend on the configurations  $\boldsymbol{\sigma}$ . For a practical

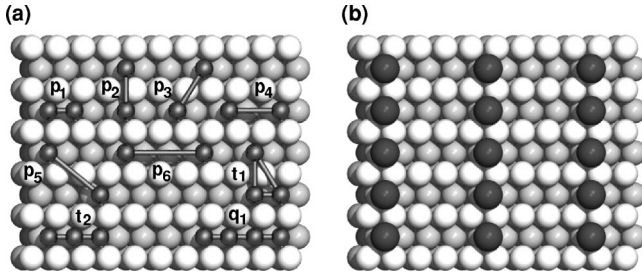


FIG. 1. (a) Top view of the volume sites on top of the Mo(112) surface which may be occupied by Li atoms. Depicted are the cluster figures which we include in our CE. (b) Top view of the Mo(112) surface covered with a  $p(4 \times 1)$  Li adatom configuration. The white and gray symbols represent Mo atoms, the black symbol Li atoms. The furrows are formed by the gray Mo atoms.

calculation, the number of clusters which are taken into account in Eq. (1) has to be confined, and therefore the convergence of the CE with respect to the number of and type of considered clusters has to be checked carefully.

The interaction parameters  $J_\alpha$  for the  $m$  clusters considered can be constructed by use of Eq. (1) from the computed energies  $E(\sigma)$  for  $n \geq m$  configurations. For  $n = m$  the  $J_\alpha$  are determined uniquely, whereas for  $n > m$  appropriate fitting procedures are used. The most reliable calculations of the energies  $E(\sigma)$  of the reference configurations is obtained by use of the *ab initio* density functional theory. The final objective is to obtain a convergence of the CE in the sense that the error arising from the termination of the series is smaller than the error involved in the *ab initio* calculations of the energies of the reference configurations. Then the energy of any conceivable configuration can be calculated very quickly from the CE with the accuracy of the *ab initio* calculations. This opens the possibility to sample very many configurations and to figure out the lowest-energy configuration for a given coverage by an appropriate search algorithm. It should be noted that the CE is a convenient mathematical representation of the energetics of the reference configurations. Clearly, the reference configurations have to be chosen carefully in order to achieve an accurate physical picture of the real physical system under consideration. For periodic reference structures the range of the clusters used in the CE is limited to clusters that are contained in the largest unit cell of the reference configurations.

As outlined above, the CE technique has been applied so far mainly to alloy and compound systems consisting of different constituent atoms. For instance, for a binary alloy  $A_x B_{1-x}$  the spin variable  $\sigma_i$  is 1 if site  $i$  is occupied by an A atom and  $-1$  if site  $i$  is occupied by a B atom. In our formalism for adatom configurations the vacant lattice site is treated as a second constituent of a binary alloy. This is indeed possible within the theory of the cluster expansion formalism without any problem, and the same idea has been used for the effect of vacancies in compounds.<sup>13</sup> Note that the substrate atoms do not appear explicitly in the cluster expansion. Their effect is contained implicitly in the energies  $E(\sigma)$  of the reference configurations.

In the following we demonstrate the power of the method for the case of Li adatom structures on the Mo(112) surface.

Kiejna and Nieminen<sup>8</sup> have calculated by *ab initio* density functional electron theory the binding energies of various configurations for different coverages, and they conclude that chain structures of Li atoms are the most favored ones in agreement with experiment. In the present paper we construct a CE from the binding energies of the reference configurations. As we will see from the CE, the information contained in the 17 reference energies can be represented by 9 quickly decaying interaction parameters.

The (112) surface of a bcc metal is furrowed along the close packed  $[11\bar{1}]$  directions, and adatoms can be absorbed along these furrows. According to the experiments,<sup>7</sup> the Li adatoms form a rectangular commensurate  $p(n \times 1)$ -type phase at coverages  $\Theta < 0.5$ , where the Li atoms occupy volume sites, i.e., positions which would be occupied by substrate atoms of an additional substrate layer. The long period ( $n$ ) is along furrows, whereas the small period is in the directions normal to the furrows so that rows normal to the furrows appear [Fig. 1(b)]. At high coverage oblique incommensurate phases are formed for which one of the overlayer axes is fixed along the furrows whereas the other is rotated out of the direction normal to the furrows. As a result, not all adatoms in the rows can occupy the energetically most favorable volume sites. The transition between commensurate and incommensurate phases has been interpreted<sup>7</sup> within the framework of an effective pair interaction model for the Li adatoms, with interactions between the adatoms in the furrows which are strongly repulsive and interaction between the adatoms in the rows which change from strongly attractive for low coverages to very weak at high coverages so that the rows can be shifted against each other rather easily.

Kiejna and Nieminen<sup>8</sup> determined by *ab initio* density functional electron theory the binding energies for various commensurate configurations (Table II of Ref. 8) at coverages  $1/8 \leq \Theta \leq 1$  which could be described by  $3 \times 1$ ,  $4 \times 1$ ,  $4 \times 2$ , and  $8 \times 1$  unit cells. Configurations with larger unit cells were not considered because the calculations are rather costly. We define the energy of formation as  $E_f = E_b(\sigma) - \Theta E_b(\Theta = 1) - (1 - \Theta) E_b(\Theta = 0)$  with the binding energy  $E_b = (1/M)(E_{\text{Li/Mo}} - E_{\text{Mo}} - N E_1)$ , where  $N$  and  $M$  denote the numbers of Li atoms and the number of sites per unit cell of the two-dimensional lattice describing the considered adatom configuration.  $E_{\text{Li/Mo}}$  is the total energy of the Mo slab with the adsorbed Li atoms,  $E_{\text{Mo}}$  is the total energy of the slab without the Li atoms, and  $E_1$  represents the total energy of an isolated Li atom. In this definition the binding energy is negative for stable adatom configurations (note that our definition has the conventional sign which is opposite to the one used by Kiejna and Nieminen<sup>8</sup>).

From the energies of formation of the reference configurations we constructed a CE including the cluster figures shown in Fig. 1(a) (a constant term and the point cluster do not contribute to  $E_f$  in a converged CE). Because the extensions of the cells of the reference configurations especially in the direction of the rows are rather small, the CE contains only short-range cluster figures. As the objective of this paper is to demonstrate the proposed CE technique for adsorbate systems at work, we refrained from performing additional *ab initio* calculations for reference configurations with

TABLE I. Values of the interaction parameters  $J_\alpha$  (in meV) for the cluster figures depicted in Fig. 1. The parameters were obtained using quadratic programming techniques based on ideas presented in Ref. 16.

$p_1$	$p_2$	$p_3$	$p_4$	$p_5$	$p_6$	$t_1$	$t_2$	$q_1$
22.55	-12.23	-3.87	6.68	1.55	1.14	-0.66	5.56	1.36

larger unit cells. Our later configuration scan then will be able to obtain for a given coverage  $\Theta$  the respective ground-state configuration for the model defined by this CE. From the fact that the  $p(4 \times 1)$  and the  $p(8 \times 1)$  structures calculated in Ref. 8 are degenerate, we conclude that long-range interactions between the chains are negligibly small. However, they may be relevant for very small coverage, where our CE, due to the limited *ab initio* input data, possibly might fail to predict the true low-coverage ground-state configurations. Finally, because only commensurate reference configurations are included, our CE will not be able to make any predictions on noncommensurate phases which—according to experiments—become relevant for  $\Theta > 0.5$ .

The values of the interaction parameters  $J_\alpha$  of our CE are given in Table I. According to Kiejna and Nieminen<sup>8</sup> the accuracy in their *ab initio* determination of the relative energies of various configurations for the same coverage is about  $\pm 5$  meV. Thus only the four largest interaction parameters of our CE exceed this error estimate. For comparison, the mean average error of the cluster expansion is 1.5 meV. The dominant interaction parameters are  $p_1$  and  $p_2$ , i.e., the pair interactions between neighboring sites along the furrows and along the rows. The parameter  $p_1$  is positive, corresponding to a repulsive interaction of neighboring Li atoms along the furrows, and it is twice as large in absolute value as the negative parameter  $p_2$  which describes an attractive interaction of neighboring Li atoms along the rows. Thus the tendency to form chainlike structures is already reflected in the values of these two parameters. The interaction parameters of the further distant pairs are either negative or positive depending on whether the corresponding distance vector has a larger component in the furrows direction or in the rows direction. The interaction parameter  $t_2$  for the triplet in furrow direction is quite large which means that the occupation of three neighboring sites in furrow direction is indeed very unfavorable.

In Fig. 2 we compare the results for the binding energies of the reference configurations for various coverages, on the one hand obtained by the *ab initio* calculations of Kiejna and Nieminen<sup>8</sup> and on the other hand determined by our CE. For all configurations the differences between the directly calculated data and the data of the CE are smaller than the error estimate of  $\pm 5$  meV for the direct calculation; i.e., the data from the CE can be considered as accurate as those from the direct calculations. Please note the asymmetry of the polygon graph connecting the data for the respective lowest-energy configurations. In the CE technique where the interaction parameters do not depend on the configurations such an asymmetry is only obtained when including cluster figures beyond the pairs. In contrast, describing the energetics by a

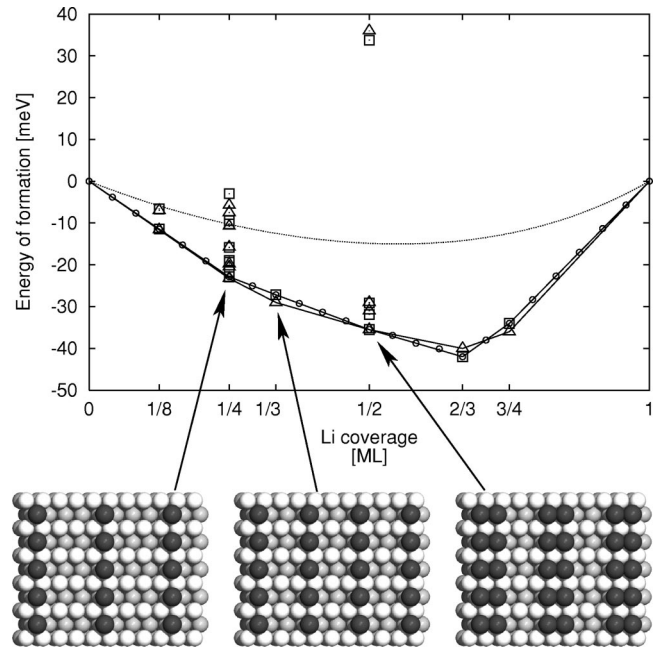


FIG. 2. Energy of formation (in meV) for different adatom configurations at different coverages  $\Theta$ . Direct *ab initio* data (Ref. 8)  $\triangle$ . Data from the CE:  $\square$ . “Extended search”:  $\circ$ . The polygon graphs connect the data for the configurations with the largest binding energies. The dashed curve represents the results obtained by the CE for a random distribution of the Li atoms on the available absorption sites. Also shown are the ground-state configurations for  $\Theta \leq 1/2$ .

model of effective pair potentials<sup>7</sup> requires to introduce pair potentials which depend on the coverage. These are just two different ways of describing energetics.

In the paper of Kiejna and Nieminen<sup>8</sup> it was attempted to find for a given coverage  $\Theta$  the configuration with the lowest energy. To do this, the energies of a small number of competing configurations (between 2 and 8) were calculated which can be described by rather small unit cells, hoping that the real ground-state configuration is among these configurations. With our CE we are now able to calculate the energies of all conceivable  $2^N$  configurations in a cell containing  $N$  sites. The ground state would be the configuration with the lowest energy for  $N \rightarrow \infty$ . Because the computing time for scanning all configurations scales with  $N$  at least with  $2^N N^2$ , the size of the considered unit cell is also limited (for larger cells more efficient search algorithms like direct minimization using linear programming techniques, Monte Carlo-simulated annealing or waiting time Monte Carlo simulations should be used). We consider  $N=24$  with different shapes of the unit cells, i.e.,  $1 \times 24$ ,  $2 \times 12$ ,  $3 \times 8$ ,  $4 \times 6$ ,  $6 \times 4$ ,  $8 \times 3$ ,  $12 \times 2$ , and  $24 \times 1$ . Among the more than  $10^8$  scanned configurations of this “extended search” are of course the few configurations considered by Kiejna and Nieminen<sup>8</sup> (configurations of the “small search”). The objective is to see whether the present “extended search” algorithm based on the CE will yield for a given coverage the same or another lowest-energy configuration as the “small search.”

The results of the “extended search” are given in Fig. 2. The figure also contains the polygon graph connecting the



CE energies for the lowest-energy configurations of the “small search.” It turns out that in the present case the lowest-energy configurations of the “small search” and the “extended search” coincide for the coverages  $\Theta$  considered by Kiejna and Nieminen<sup>8</sup> (of course, this might be different for other systems). We find a  $p(4 \times 1)$  ground-state structure for  $\Theta = 1/4$ , a  $p(3 \times 1)$  phase at  $\Theta = 1/4$ , and pairs of Li chains in a  $(4 \times 1)$  unit cell at  $\Theta = 1/2$ . Furthermore, for other coverages  $\Theta$  the “extended search” yields energies for the lowest-energy configuration which coincide with the energy of the polygon graph at that  $\Theta$  or which are located above the polygon graph. In the latter case, a heterogeneous mixture of the two phases which belong to the two neighboring corner points of the polygon graph is more favorable than the respective homogeneous lowest-energy configurations. For coverages  $\Theta_m = m/N_r$ ,  $m = 1, 2, \dots, N_r$ , with  $N_r$  characterizing the length of the unit cell of the “extended search” in the row direction perpendicular to the furrows, the lowest-energy configurations consist of the infinitely extended rows already identified by the “small search.” Obviously, the large attractive interaction  $p_2$  always drives the formation of chainlike structures perpendicular to the furrows and therefore within the present CE the lowest-energy configurations are arrangement of Li chains. It might well be that for a readily converged CE constructed from reference configurations with larger unit cells other lowest-energy configurations could be identified for some  $\Theta$ , like, e.g.,  $\Theta < 1/8$  with energies below the polygon graph. Note that the

phase diagram reported in Ref. 7 does not contain the ground-state structures found in the present work at  $\Theta = 1/3$  and  $\Theta = 1/2$ . As can be seen from Fig. 2, the ground state at  $\Theta = 1/3$  lies only slightly under the direct line connecting the ground states at  $\Theta = 1/4$  and  $\Theta = 1/2$ , giving the possibility that this ground state cannot be observed at the experimental measuring temperature of more than 100 K. On the other hand, the *ab initio*-calculated energy differences in Ref. 8 between the experimentally observed  $p(2 \times 1)$  and the  $\Theta = 1/2$  ground-state structure discussed above are very small, so that the *ab initio* calculations might fail to predict the correct energetic order.

To conclude, we have demonstrated that the CE technique provides an efficient tool with the accuracy of the *ab initio* electron theory to figure out the ground-state configurations formed by adatoms on plane substrate surfaces in thermal equilibrium, thereby condensing the information essentially contained in the energetics into few descriptive interaction parameters. By combination with the cluster-variation method<sup>9,14</sup> or with Monte Carlo simulations the CE method could be also used to predict the equilibrium phase diagram as a function of temperature  $T$  and coverage  $\Theta$ . Finally, the CE technique has been also used in the context of kinetic Monte Carlo simulations<sup>15</sup> for the growth of precipitates in alloys. With the version of the CE technique described in the present report kinetic Monte Carlo simulations can be also applied to describe the metastable adatom configurations formed by diffusion-controlled aggregation.<sup>5</sup>

\*Electronic address: faehn@physix.mpi-stuttgart.mpg.de

<sup>1</sup>F.J. Himpsel, J.E. Ortega, G.J. Mankey, and R.F. Willis, *Adv. Phys.* **47**, 511 (1998).

<sup>2</sup>H.W. Yeom, S. Takeda, E. Rotenberg, I. Matsuda, K. Horikoshi, J. Schaefer, C.M. Lee, S.D. Kevan, T. Ohta, T. Nagao, and S. Hasegawa, *Phys. Rev. Lett.* **82**, 4898 (1999).

<sup>3</sup>P. Gambardella, A. Dallmeyer, K. Maiti, M.C. Malagoli, W. Eberhardt, K. Kern, and C. Carbone, *Nature (London)* **416**, 301 (2002).

<sup>4</sup>R. Bennewitz, J.N. Crain, A. Kirakosian, J.-L. Lin, J.L. McChesney, D.Y. Petrovykh, and F.J. Himpsel, *Nanotechnology* **13**, 499 (2002).

<sup>5</sup>H. Röder, E. Hahn, H. Brune, J.-P. Bucher, and K. Kern, *Nature (London)* **366**, 141 (1993).

<sup>6</sup>P. Fernandez, C. Massobrio, P. Blandin, and J. Buttet, *Surf. Sci.* **307**, 608 (1994).

<sup>7</sup>A. Fedorus, D. Kolthoff, V. Koval, I. Lyuksyutov, A.G. Naumovets, and H. Pfnür, *Phys. Rev. B* **62**, 2852 (2000).

<sup>8</sup>A. Kiejna and R.M. Nieminen, *Phys. Rev. B* **66**, 085407 (2002).

<sup>9</sup>J.M. Sanchez, F. Ducastelle, and D. Gratias, *Physica A* **128**, 334

(1984).

<sup>10</sup>*Statics and Dynamics of Alloy Phase Transformations*, Vol. 319 of *NATO Advanced Study Institute, Series B: Physics*, edited by P.E.A. Turchi and A. Gonis (Plenum, New York, 1994).

<sup>11</sup>R. Drautz, H. Reichert, M. Fähnle, H. Dosch, and J.M. Sanchez, *Phys. Rev. Lett.* **87**, 236102 (2001).

<sup>12</sup>C. Stampfl, H.J. Kreuzer, S.H. Payne, H. Pfnür, and M. Scheffler, *Phys. Rev. Lett.* **83**, 2993 (1999); C. Stampfl, H.J. Kreuzer, S.H. Payne, and M. Scheffler, *Appl. Phys. A: Mater. Sci. Process.* **69**, 471 (1999); K.A. Fichthorn and M. Scheffler, *Phys. Rev. Lett.* **84**, 5371 (2000); K.A. Fichthorn, M.L. Merrick, and M. Scheffler, *Appl. Phys. A: Mater. Sci. Process.* **75**, 17 (2002).

<sup>13</sup>C. Wolverton and A. Zunger, *Phys. Rev. Lett.* **81**, 606 (1998); G. Ceder and A. Van der Ven, *Electrochim. Acta* **45**, 131 (1999); F. Lechermann and M. Fähnle, *Phys. Rev. B* **63**, 012104 (2001).

<sup>14</sup>R. Kikuchi, *Phys. Rev.* **81**, 988 (1951); *J. Chem. Phys.* **60**, 1071 (1974).

<sup>15</sup>S. Müller, L.-W. Wang, and A. Zunger, *Modell. Simul. Mater. Sci. Eng.* **10**, 131 (2002).

<sup>16</sup>A. van der Walle and G. Ceder, *J. Phase Equilib.* **23**, 348 (2002).